Common-Resolution Convolution Kernels for Space- and Ground-Based Telescopes.

Spitzer, Herschel, GALEX, WISE, Moffat functions, and multi/single Gaussian PSFs.

Gonzalo J. Aniano Porcile, Bruce Draine, Karl Gordon and Karin Sandstrom.
ganiano@astro.princeton.edu http://www.astro.princeton.edu/$\sim$ganiano/Kernels.html

Abstract

Multi-wavelength study of extended astronomical objects requires combining images from instruments with differing point spread functions (PSFs).
We constructed convolution kernels that allow one to generate (multi-wavelength) images with a common PSF, thus preserving the colors of the astronomical sources. We generate convolution kernels for the cameras of the Spitzer Space Telescope, Herschel Space Observatory, Galaxy Evolution Explorer (GALEX), Wide-field Infrared Survey Explorer (WISE), ground-based optical telescopes (Moffat functions and sum of Gaussians), and Gaussian PSFs. These kernels allow the study of the Spectral Energy Distribution (SED) of extended objects, preserving the characteristic SED in each pixel.
The convolution kernels and the IDL packages used to construct and use them are made publicly available.

Convolution Kernels

Given two cameras A and B, with (different) PSFs Ψ_A and Ψ_B, the images obtained of an astronomical object will, even if the spectral response of the cameras were identical, be different. A convolution kernel is a tool that transforms the image observed by one camera into an image corresponding to the PSF of another camera. The convolution kernel $K_{A\Rightarrow B}$ from camera A to camera B should satisfy:

$$I_B(x,y) = \int\int I_A(x',y') K_{A\Rightarrow B}(x-x', y-y') dx' dy',$$

where I_A and I_B are the observed images by the cameras A and B respectively. We can easily invert this equation in Fourier space:

$$K_{A\Rightarrow B} = FT^{-1}\left(FT(\Psi_B) \times \frac{1}{FT(\Psi_A)}\right),$$

where FT and FT^{-1} stand for the Fourier transform and its inverse transformation respectively. Several Filters are applied (see [1]).

Kernel Performance

We generated the kernels $K_{A\Rightarrow B}$ for all appropriate combinations (A,B). We compute $\Psi_A \star K_{A\Rightarrow B}$, and compare it with Ψ_B.
One measure of kernel performance is its accuracy in redistribution of PSF power. We define:

$$D = \int\int | \Psi_B - K_{A\Rightarrow B} \star \Psi_A | dxdy.$$

A second quantitative measure of kernel performance is obtained by studying its negative values. We define:

$$W_{\pm} = \frac{1}{2}\int\int (| K_{A\Rightarrow B} | \pm K_{A\Rightarrow B})\, dxdy$$

On [1] we studied the performance of all the kernels generated. For example:

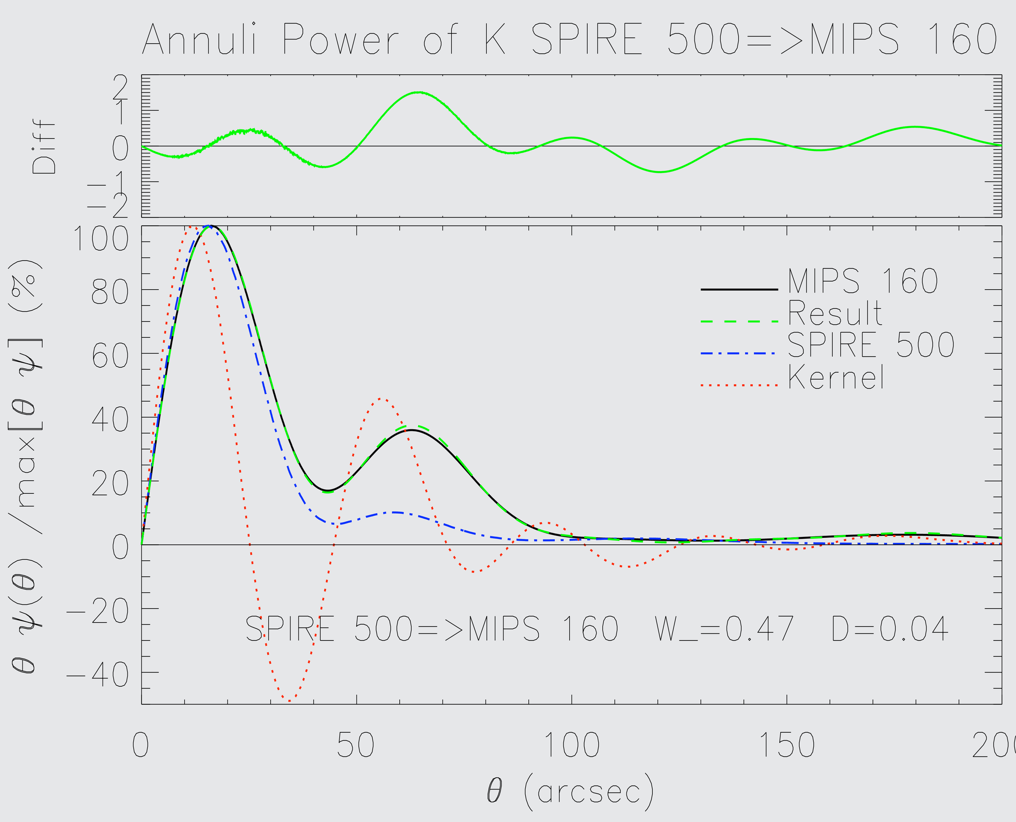

PSFs

In-flight instrumental PSFs:

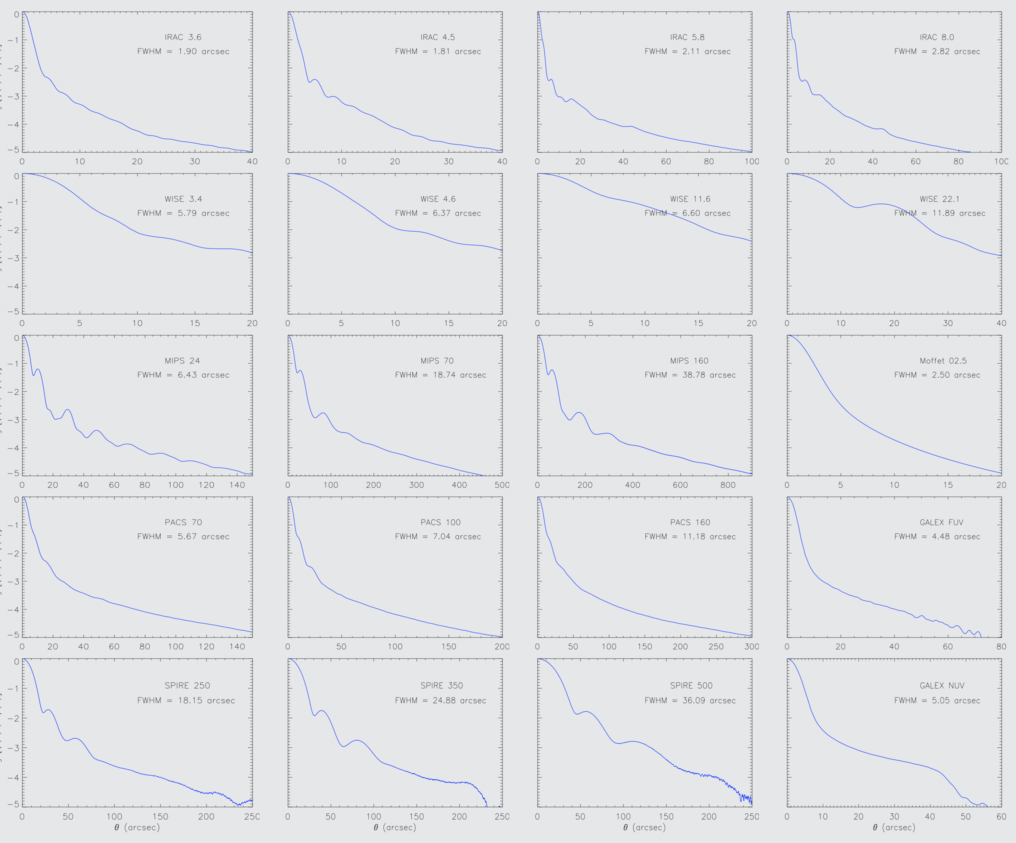

Camera	Rayleigh diff. limit[a] (arcsec)	Measured FWHM (arcsec)	99% of energy radius (arcsec)	κ[b]	Asymmetry g[c]
IRAC 3.6μm	1.04	1.90	62.52	1.29	0.16
IRAC 4.5μm	1.31	1.81	64.46	1.26	0.17
IRAC 5.8μm	1.68	2.11	133.55	1.20	0.19
IRAC 8.0μm	2.30	2.82	114.20	1.19	0.18
MIPS 24μm	6.93	6.43	224.53	1.05	0.08
MIPS 70μm	20.90	18.74	461.44	1.12	0.05
MIPS 160μm	45.62	38.78	678.77	1.10	0.05
PACS 70μm	5.11	5.67	249.81	1.23	0.20
PACS 100μm	7.28	7.04	350.63	1.19	0.20
PACS 160μm	11.70	11.18	417.36	1.21	0.20
SPIRE 250μm	17.93	18.15	205.07	1.16	0.19
SPIRE 350μm	25.16	24.88	192.47	1.15	0.18
SPIRE 500μm	36.22	36.09	198.43	1.16	0.19
GALEX FUV	0.08	4.48	50.28	1.26	0.07
GALEX NUV	0.11	5.05	39.56	1.32	0.05
WISE 3.35μm	2.11	5.79	19.10	1.20	0.17
WISE 4.60μm	2.89	6.37	19.08	1.33	0.13
WISE 11.56μm	7.27	6.60	19.56	1.23	0.12
WISE 22.1μm	13.90	11.89	35.15	1.05	0.07
Gauss 12″		12.00	15.41	1.33	0.0
Gauss 20″		20.00	25.68	1.33	0.0
Gauss 23″		23.00	29.53	1.33	0.0
Gauss 28″		28.00	35.95	1.33	0.0
Gauss 40″		40.00	51.33	1.33	0.0
Gauss 50″		50.00	64.05	1.33	0.0
BiGauss 0.5″		0.50	0.90	1.37	0.0
BiGauss 1.0″		1.00	1.79	1.37	0.0
BiGauss 1.5″		1.50	2.69	1.37	0.0
BiGauss 2.0″		2.00	3.57	1.37	0.0
BiGauss 2.5″		2.50	4.44	1.37	0.0
Moffat 0.5″		0.50	1.39	1.46	0.0
Moffat 1.0″		1.00	2.77	1.46	0.0
Moffat 1.5″		1.50	4.12	1.46	0.0
Moffat 2.0″		2.00	5.45	1.46	0.0
Moffat 2.5″		2.50	6.74	1.46	0.0

[a] We take Rayleigh diffraction limit = 1.22 × [central λ] / [telescope diameter].
[b] $\kappa = (k_H \times \mathrm{FWHM}_A)/(2\pi)$ where k_H is the high frequency cutoff (see text for details).
[c] g is a measure of the departure of a PSF from rotational symmetry (see equation (12)).

Ground-based optical and radio telescopes:

- Gaussians: $\Psi(\theta) = \frac{1}{2\pi\sigma^2}\exp\left(\frac{-\theta^2}{2\sigma^2}\right)$, with $5'' < \mathrm{FWHM} < 60''$.
- Optical: $\Psi(\theta) = 0.9\frac{1}{2\pi\sigma^2}\exp\left(\frac{-\theta^2}{2\sigma^2}\right) + 0.1\frac{1}{2\pi(2\sigma)^2}\exp\left(\frac{-\theta^2}{2(2\sigma)^2}\right)$
with FWHM = 0.5, 1.0, 1.5, 2.0, 2.5″.
- Optical: $M_\beta(\theta) = \frac{(\beta-1)(2^{1/\beta}-1)}{\pi\,\theta_0^2}\left[1+(2^{1/\beta}-1)\left(\frac{r}{\theta_0}\right)^2\right]^{-\beta}$
PSFs are of the form: $\Psi(r) = 0.8\times M_7(\theta) + 0.2\times M_2(\theta)$,
with $\mathrm{FWHM} = 2\,\theta_0 = 0.5, 1.0, 1.5, 2.0, 2.5''$.

Example: $K_{\mathrm{MIPS24}\Rightarrow\mathrm{SPIRE250}}$

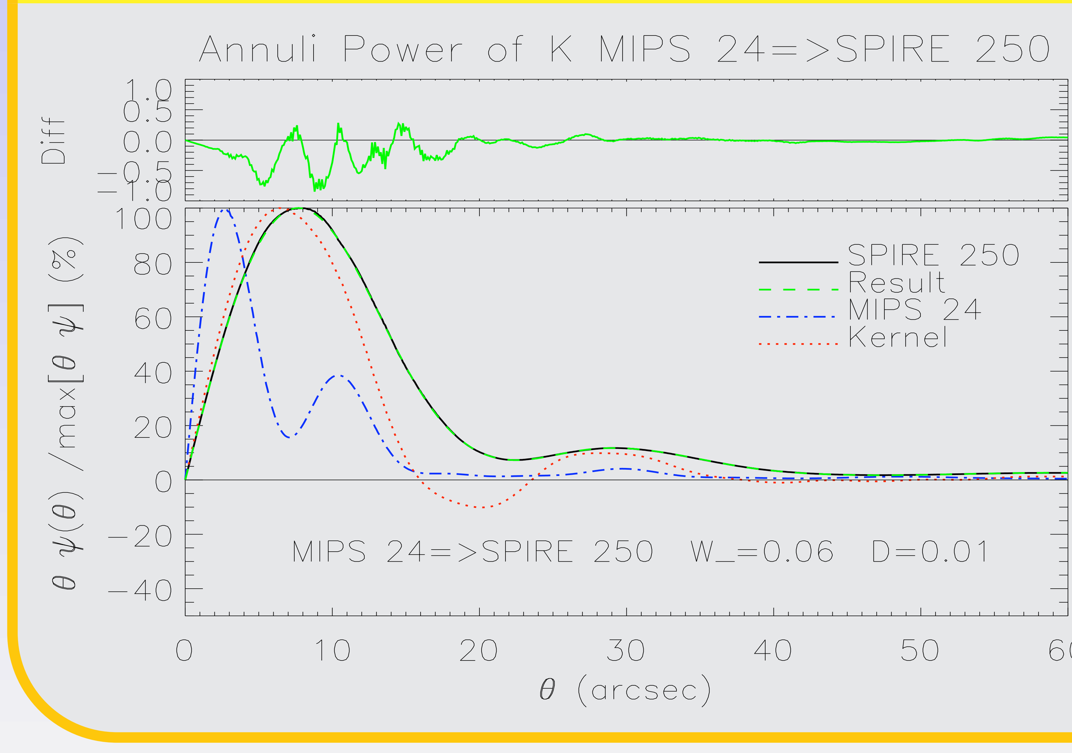

Example: NGC1097

Herschel and Spitzer images convolved to SPIRE250μm PSF:

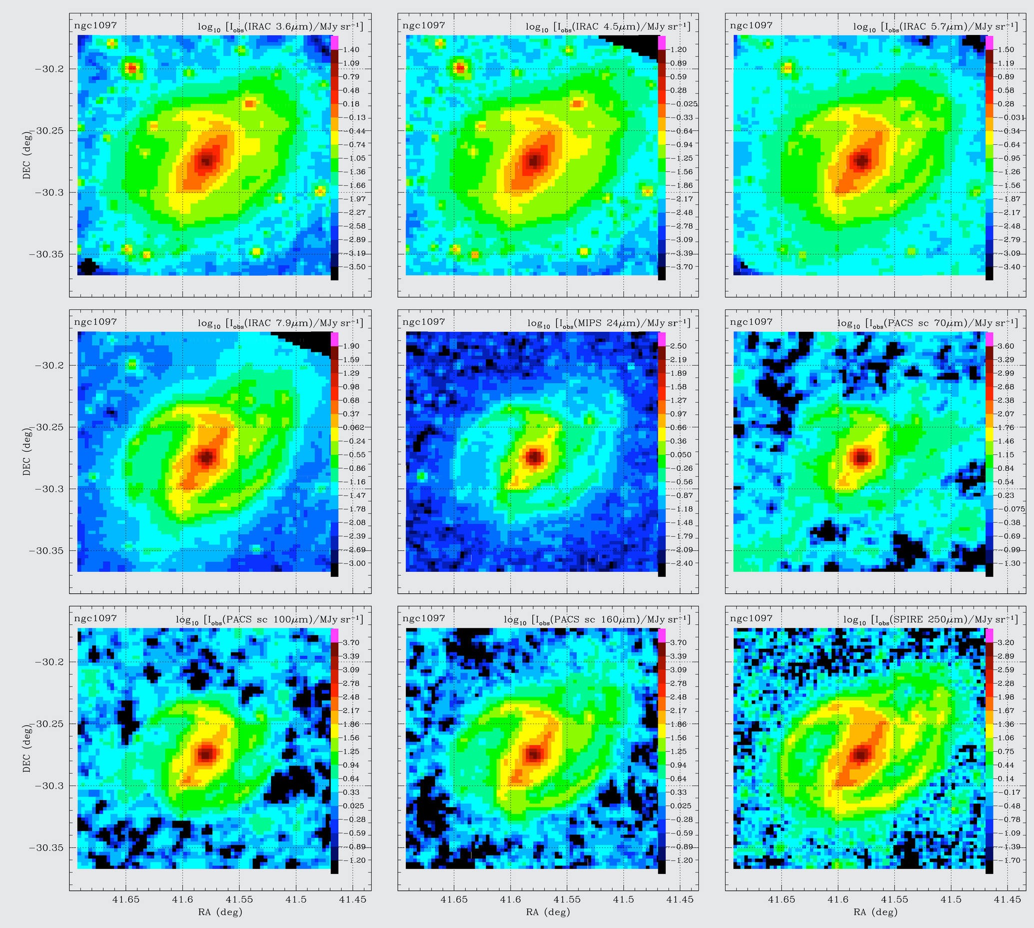

Fig. 9.— Spitzer and Herschel images of NGC1097 convolved to a SPIRE 250μm PSF. The SPIRE 250μm camera was convolved with the kernel $K_{\mathrm{SPIRE250}\Rightarrow\mathrm{SPIRE250}}$. The color bar has the same dynamic range ($10^{4.9}$) for all images.

SPIRE 250μm convolved:

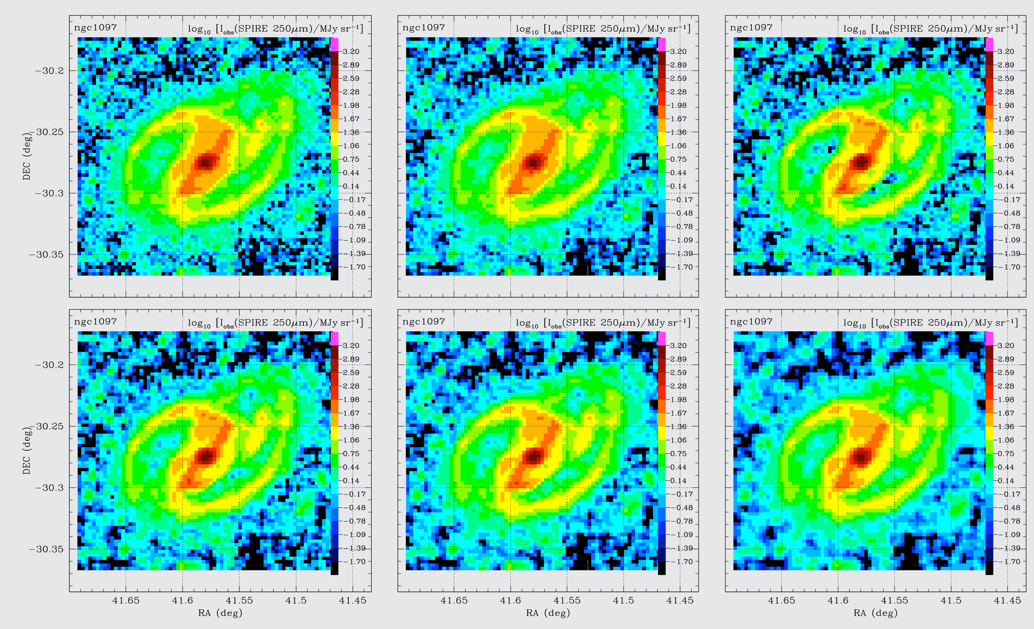

Fig. 10.— SPIRE 250μm image of NGC1097. Top row left: original SPIRE image; center: image convolved with $K_{\mathrm{SPIRE250}\Rightarrow\mathrm{SPIRE250}}$; extremely aggressive convolution to a Gaussian PSF with FWHM = 18″ ($W_- = 1.47$). Bottom row: image convolved with suitable Gaussian PSFs: left (aggressive) FWHM = 19″ ($W_- = 1.05$); center (moderate) FWHM = 21″ ($W_- = 0.44$); right (very safe) FWHM = 22″ ($W_- = 0.30$). All the images have the same color bar.

Optimal Gaussian PSFs

For each instrumental PSF we found a set of optimal Gaussian PSF.
The first FWHM is obtained by requiring that $W_- \sim 0.3$, giving a conservative (very safe) kernel that does not seek to move too much energy from the wings into the main Gaussian core, at the cost of having a larger FWHM (i.e., lower resolution).
The second FWHM has $W_- \sim 0.5$, and we consider it to be a good (moderate) Gaussian FWHM to use.
The third FWHM has $W_- \sim 1.0$.

Table 6: Gaussian FWHM suitable for each camera.

Camera	Actual FWHM (″)	Aggressive Gaussian with $W_- \approx 1.0$		Moderate Gaussian with $W_- \approx 0.5$		Very safe Gaussian with $W_- \approx 0.3$	
		FWHM (″)	W_-	FWHM (″)	W_-	FWHM (″)	W_-
MIPS 24μm	6.5	8.0	1.00	11.0	0.49	13.0	0.30
MIPS 70μm	18.7	22.0	1.01	30.0	0.51	37.0	0.30
MIPS 160μm	38.8	46.0	1.01	64.0	0.50	76.0	0.30
PACS 70μm	5.8	6.5	0.84	8.0	0.48	10.5	0.31
PACS 100μm	7.1	7.5	1.10	9.0	0.52	12.5	0.31
PACS 160μm	11.2	12.0	1.05	14	0.50	18.0	0.33
SPIRE 250μm	18.2	19.0	1.05	21.0	0.44	22.0	0.30
SPIRE 350μm	25.0	26.0	0.98	28.0	0.50	30.0	0.27
SPIRE 500μm	36.4	38.0	0.96	41.0	0.48	43.0	0.30

References

[1] Aniano, G., Draine, B., Gordon, K., Sandstrom, K., PASP, submitted, (see Tuesday's astro-ph: arXiv:1106.5065)